The Lipopolysaccharide Barrier: Correlation of Antibiotic Susceptibility with Antibiotic Permeability and Fluorescent Probe Binding Kinetics†

D. Scott Snyder‡ and Thomas J. McIntosh*

Department of Cell Biology, Duke University Medical Center, Durham, North Carolina 27710

Received April 11, 2000

ABSTRACT: Lipopolysaccharide (LPS), the primary lipid on the surface of Gram-negative bacteria, is thought to act as a permeability barrier, making the outer membrane relatively impermeable to hydrophobic antibiotics, detergents, and host proteins. Mutations in the LPS biosynthetic apparatus increase bacterial susceptibility to such agents. To determine how this increased susceptibility is mediated, we have correlated antibiotic susceptibilities of rough (antibiotic resistant) and deep rough (antibiotic susceptible) bacterial strains with antibiotic permeabilities and fluorescent probe binding kinetics for bilayers composed of LPS purified from the same strains. Bilayer permeabilities of two hydrophobic β-lactam antibiotics were measured by encapsulating the appropriate β-lactamases in large unilamellar vesicles. In the presence of $MgCl_2$, permeabilities of LPS bilayers from rough and deep rough bacteria were similar and significantly lower than those of bacterial phospholipids (BPL). Addition of BPL to the LPS bilayers increased their antibiotic permeability to approximately the level of the BPL bilayers. Binding rates of the fluorescent probe bis-aminonaphthylsulfonic acid (BANS) were 2 orders of magnitude slower for both rough and deep rough LPS bilayers compared to that of bilayers composed of BPL or mixtures of LPS and BPL. On the basis of these results and the observation that deep rough bacteria have higher levels of phospholipid on their surface than do rough bacteria (Kamio, Y., and Nikaido, H. (1976) *Biochemistry 15,* 2561−2569), we argue that the high susceptibility of deep rough bacteria is due to the presence of phospholipids on their surface. Experiments with phospholipid bilayers showed that the addition of PEG−lipids (containing covalently attached hydrophilic polymers) had little effect on permeability and binding rates, whereas the addition of cholesterol reduced permeability and slowed binding to levels approaching those of LPS. Therefore, we argue that the barrier provided by LPS is primarily due to its tight hydrocarbon chain packing (Snyder et al., (1999) *Biochemistry 38,* 10758−10767) rather than to its polysaccharide headgroup.

Gram-negative bacteria surround themselves with a double membrane. The inner, or cytoplasmic, membrane is composed of phospholipids, whereas the outer membrane is an asymmetric structure containing primarily phospholipids in its inner monolayer and lipopolysaccharide (LPS[1]) in its outer monolayer. LPS differs in structure from phospholipids in that it uses sugar residues for its backbone, can have up to seven fatty acids per molecule, and has a sizable saccharide chain extending from the lipid backbone (Figure 1). It is known that Gram-negative bacteria are less susceptible and their surfaces are less permeable than those of Gram-positive bacteria to specific antibiotics (*1, 2*). LPS is thought to be a major factor in this permeability reduction, at least to large hydrophobic molecules (*1*). Certain mutations which render the bacteria unable to complete the addition of the oligosaccharide chain or to add certain polar substituents (such as pyrophosphate and phosphoethanolamine) cause the bacteria to lose their natural resistance to antibiotics and to display a series of characteristics which are known as the deep rough phenotype (Figure 1) (*3*, *4*). This is in contrast to the rough and smooth phenotypes (Figure 1), which are more resistant to hydrophobic antibiotics (*3*). Among the rough and deep rough phenotypes are a number of chemotypes with different number of sugars on their saccharide cores. For example, the LPS of the Ra chemotype has a complete saccharide core without O-antigen, the Rc chemotype is unable to add sugars beyond the first glucose, and the Rd chemotype is unable to add even the first glucose (Figure 1).

Several hypotheses involving the permeability properties of LPS have been presented to explain the differences in hydrophobic antibiotic susceptibilities between rough and deep rough chemotypes. These hypotheses utilize various structural differences between LPS and phospholipids to explain the function of LPS as a permeability barrier.

The first hypothesis states that the barrier properties of LPS are mediated through its carbohydrate chain, which acts as a hydrophilic shield to prevent the passage of hydrophobic

† This work was supported by Grants GM27278 and GM58432 from the National Institutes of Health.

* To whom correspondence should be addressed. Telephone: 919-684-8950. Fax: 919-681-9929. E-mail: T.McIntosh@cellbio.duke.edu.

‡ Present address: Rocky Mountain Laboratories, NIH, NIAID, 903 Fourth Street, Hamilton, MT 59840.

[1] Abbreviations: LPS, lipopolysaccharide; BPL, bacterial phospholipids; PEG, poly(ethylene glycol); T_m, gel to liquid-crystalline phase transition temperature; BANS, bis-aminonaphthylsulfonic acid; PC, phosphatidylcholine; DMPC, dimyristoylphosphatidylcholine; SM, bovine sphingomyelin; PEG−lipid, 1,2-distearoyl-*sn*-glycerol-3-phosphoethanolamine−*N*-poly(ethylene glycol) 2000; PVP, poly(vinylpyrrolidone); SRB, sulforhodamine B; LUV, large unilamellar vesicle.

10.1021/bi000810n CCC: $19.00
Published on Web 08/25/2000

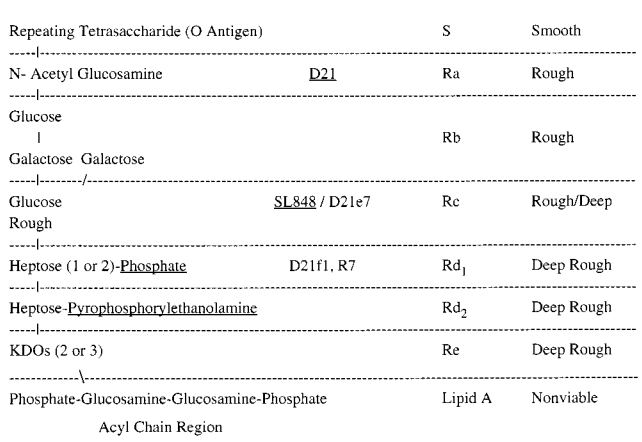

FIGURE 1: Generalized structure of the LPS molecules used in this paper. The phenotype names (smooth and rough) refer to the appearance of the bacterial colonies growing on agar plates. Lipid A contains a diglucosamine backbone and an acyl chain region usually containing six or seven fatty acids. The "core" saccharide region extends from the lipid A moiety to the repeating tetrasaccharide (O-antigen) region found in smooth bacteria. The core contains a variable number of sugars depending on the chemotype. The phosphate and pyrophosphorylethanolamine polar substituents on the inner core heptoses are present in the underlined Ra (D21) and RcP^+ (SL848) strains but not in the RcP^- (D21e7) and RdP^- (D21f1 and R7) strains.

molecules (*4*, *5*). Previous X-ray diffraction results have shown that LPS bilayers do possess a hydrophilic barrier whose width depends on the number of saccharides in the LPS core (*6*). Related to this hypothesis, steric barriers have also been observed and measured for liposomes containing phospholipids with covalently attached poly(ethylene glycol) chains (PEG−lipids) (*7*−*9*). The magnitude and width of this steric barrier depend on the size of the attached polymer (*7*−*9*), and the PEG−lipids can prevent the access of large, but not small, amphipathic molecules to the bilayer surface (*10*).

A second hypothesis holds that LPS molecules in the outer membrane are tightly linked through a series of intermolecular crossbridges with divalent cations (*3*). In support of this, it has been noted that divalent cations decrease the antibiotic hypersusceptibility of deep rough strains of bacteria (*11*) and EDTA is known to enhance the uptake of β-lactams (*3*), presumably by binding divalent cations. The observation that isolated LPS has high levels of bound divalent cations (*12*) underscores the importance of understanding the role of divalent cations in mediating LPS properties.

Parker et al. (*13*) have proposed that LPS molecules may bind to one another by hydrogen bonding and possibly ionic interactions between polar substituents such as phosphoethanolamine. In contrast to the metal cross-bridging hypothesis, no cations need be present for this interaction to work. According to this hypothesis, the buildup of phosphatidylethanolamine in the outside monolayer is actually a form of precursor buildup as these molecules can act as donors of phosphoethanolamine moieties to LPS (*14*).

Brandenburg and Seydel (*15*) have proposed that the permeability barrier function of LPS is related to its gel to liquid-crystalline phase-transition temperature (T_m), which is quite high compared to those of typical eukaryotic membrane lipids. These authors (*15*, *16*) have found a sequential decrease in T_m with decreasing core length. The smooth form LPS was found to have a T_m of approximately 37−38 °C, as measured by several different methods, whereas Ra LPS has a T_m of 36−38 °C and Re has a T_m of 30−32 °C. However, the Rc and Rd chemotypes, whose parent strains differ greatly in their susceptibility to antibiotics, have about the same T_m at 33−35 and 32−33 °C, respectively. The presence of $MgCl_2$ increases the phase-transition temperature of deep rough LPSs but has little effect on Ra LPS (*16*).

A final hypothesis (*4*, *17*, *18*) states that the increased permeability of the deep rough mutants is due to presence of phospholipids in the outer monolayer of the outer membrane. Kamio and Nikaido (*19*) found that deep rough mutants have a larger amount of phospholipids in their outer monolayer (about 30 area %) than does rough or smooth bacteria. Roantree et al. (*20*) argue that hydrophobic antibiotics can gain access in deep rough strains when phospholipid patches appear in the outer monolayer. Plesiat and Nikaido (*21*) also note that deep rough mutants, which have higher permeability for hydrophobic solutes, have fewer porins in their outer membranes, but perhaps more phospholipids.

A systematic test of these sometimes competing and sometimes complementary hypotheses has not been undertaken. In particular, although there have been a number of susceptibility studies of mutant bacteria to various antibiotics (*3*, *4*, *20*), there have been few permeability measurements with LPS bilayers nor thorough correlations of bacterial susceptibilities with LPS permeabilities. It is our goal to test the above hypotheses by determining the permeability of bilayers composed of LPSs obtained from bacteria with a range of susceptibilities to hydrophobic antibiotics. Such experiments with symmetric LPS bilayers should have relevance to the asymmetric outer membrane of Gram-negative bacteria as permeability studies of both planar lipid bilayers (*22*) and single-walled lipid vesicles (*22*, *23*) have shown that the apposing monolayers in a lipid bilayer offer independent resistances to permeation, with the overall permeability being a function of the sum of resistances exerted by the two monolayers.

We have chosen three antibiotics for susceptibility measurements: novobiocin, cephaloridine, and nitrocefin. The largest, novobiocin, has sufficient size (molecular weight 634 Da) so that it unlikely to pass through outer membrane porin channels which are permeable to hydrophilic solutes of less than about 600 Da (*4*, *17*, *20*). Novobiocin is known to affect deep rough mutants more strongly than it does rough mutants (*20*), but unfortunately, it cannot be used for permeability assays because no real-time assays exist for its presence. However, the β-lactam antibiotics cephaloridine and nitrocefin can be tested in real-time degradation assays. Cephaloridine, with a molecular weight of 415 Da, passes through porin channels in vivo (*24*); thus it should show no difference in susceptibility for mutants of differing bilayer permeability and allows us to gauge any intrinsic susceptibility differences among the bacterial strains. Cephaloridine has previously been tested for permeability (*5*) and is degradable by penicillinase isolated from *Enterobacter cloacae.* Unfortunately, both this enzyme and the iodine-based assay mix used to monitor its degradation are unstable at temperatures over 37 °C, preventing measurements of Ra LPS permeability in its liquid-crystalline phase. However, we have found that

nitrocefin is degradable by the *B. cereus* type II β-lactamase which is stable at more elevated temperatures, thereby allowing measurements of Ra LPS permeability. Nitrocefin is large enough (molecular weight 516 Da) to potentially impede its flow through porin channels.

To further analyze the efficacy of the permeability barrier provided by different LPS chemotypes, we have analyzed the kinetics of binding of the membrane fluorescent probe bis-aminonaphthylsulfonic acid (BANS). BANS is essentially nonfluorescent in water but becomes fluorescent upon entering a hydrophobic environment, such as the hydrocarbon core of a lipid bilayer. By monitoring fluorescence increase with time, rates of binding for this molecule can be established. Such kinetic data can be used to analyze the mechanism of probe−bilayer interactions in terms of chemical reactions representing binding and transbilayer movement (*25*, *26*). BANS has physical properties similar to those of the tested antibiotics, as it is hydrophobic and has a similar molecular weight (672 Da). Therefore, we argue that the forces governing the kinetics of BANS binding should be similar to those of the three antibiotics studied in this paper.

To provide additional information on the structural factors involved in the LPS permeability barrier, we have compared permeability and binding kinetics for LPS bilayers with bilayers composed of several types of phospholipids, including total bacterial phospholipids (BPL), phosphatidylcholine (PC), PC/cholesterol, and PC/cholesterol containing phospholipids with covalently attached poly(ethylene glycol) (PEG−lipids). Experiments with cholesterol, which is known to reduce area per lipid molecule, provide information on the effects of lipid packing, whereas experiments with the PEG−lipids test the role of a hydrophilic barrier in modifying permeability and binding kinetics of hydrophobic molecules.

MATERIALS AND METHODS

Materials. LPS samples were either purchased from Sigma Chemical Corp. (St. Louis, MO), as in the case of the *S. minnesota* R7, or extracted from bacteria, as in the case of *E. coli* D21, D21e7, and D21f1, and *S. typhimurium* SL848. *E. coli* bacterial strains were obtained from Dr. J. A. Fralick, Texas Tech University Health Sciences Center (Lubbock, TX) and the *E. Coli* Genetic Stock Center at Yale University (New Haven, CT), and *S. typhimurium* SL848 was obtained from Salmonella Genetics Stock Center (Calgary, Alberta, Canada). LPS extractions were performed using a phenol/chloroform/petroleum ether extraction (*27*), together with an acetone precipitation and ethanol washing procedure (*28*). Briefly, ether powders of ethanol-extracted cells were extracted with phenol/chloroform/petroleum ether 2:5:8 (v:v:v) and then centrifuged to remove unwanted material. The extraction solution was then dried with a rotary evaporator to remove chloroform and petroleum ether after which acetone and diethyl ether were added to precipitate the LPS.

Total *E. coli* lipid extract, dimyristoylphosphatidylcholine (DMPC), bovine sphingomyelin (SM), and PEG−lipid (1,2-distearoyl-*sn*-glycerol-3-phosphoethanolamine−*N*-poly(ethylene glycol) 2000) were purchased from Avanti Polar Lipids (Alabastar, AL), novobiocin, cephaloridine, *E. coli* cardiolipin, poly(vinylpyrrolidone) (PVP), and cholesterol were purchased from Sigma Chemical Corp., nitrocefin was purchased from Oxoid (Hampshire, England) and Calbiochem (LaJolla, CA), and BANS was purchased from Molecular Probes (Eugene, OR). For controls in permeability experiments, the bacterial phospholipids (BPL) were supplemented with 4 mol % cardiolipin to be consistent with the work of Hiruma et al. (*5*). *E. cloacae* β-lactamase was obtained from Sigma, and *B. cereus* type II β-lactamase was the kind gift of Dr. Moreno Galleni, Centre d'Ingenierie des Proteines, Liege, Belgium.

LPS Salt Removal and Acidification. To ensure that the LPS was in a single defined salt form, an EDTA/HCl washing procedure was used. Briefly, LPS in a solution of 20 mM TEA-EDTA pH 7.0 was sonicated in a bath sonicator, mixed with 2.5 vol of 2:1 chloroform/methanol, vortexed, and centrifuged to separate the aqueous and organic phases. The organic phase containing most of the LPS was transferred to fresh tubes with 0.4 vol of methanol and 0.6 vol of 0.1 N HCl. The resulting mixture was centrifuged, and the organic phase was removed for drying. To recover LPS in the interfacial regions, as well as any left in the aqueous phases, both aqueous phases were re-extracted with 2.5 vol of fresh chloroform. That is, chloroform was added first to the aqueous phase of the EDTA extraction, vortexed, centrifuged, and removed and then added to the acid aqueous phase, vortexed, centrifuged, and removed for drying. This re-extraction procedure was repeated, using fresh chloroform each time, until no visible interface was present. Organic phases were combined and dried under nitrogen. This procedure produced LPS in its acid form, which was converted to either a sodium or partial magnesium salt by resuspension in 20 mM HEPES, 10 mM EDTA, and 90 mM NaCl, pH 7.0, or 20 mM HEPES, 0.5 mM $MgCl_2$, and 90 mM NaCl, pH 7.0, respectively. For experiments involving mixtures of LPS and phospholipids, the acid form LPS and phospholipid were mixed in organic phase and dried under nitrogen before resuspension in the appropriate buffer.

Antibiotic Susceptibility Testing. Antibiotic susceptibility testing was performed by the Macrodilution Broth Method as specified by the National Committee for Clinical Laboratory Testing *(29*). We used Mueller Hinton broth supplemented with 20 mM $MgCl_2$. Briefly, 2-fold serial dilutions of each antibiotic were done beginning at 512 ug/mL and ending at 0.125 ug/mL. To each tube, 500 000 colony-forming units (CFU) of bacteria were added and incubated at 37 °C for 16−20 h. The minimum inhibitory concentration was taken as the lowest concentration of antibiotic that inhibited growth of the organism as detected by the unaided eye.

Sulforhodamine B Encapsulation. Dried LPS or phospholipid (2−5 mg) was suspended in 0.5 mL of 20 mM HEPES, 10 mM EDTA and 90 mM NaCl, pH 7.0, or 20 mM HEPES, 0.5 mM $MgCl_2$, and 90 mM NaCl, pH 7.0, containing 10 mM Sulforhodamine B (SRB), a concentration of SRB which is virtually nonfluorescent due to self-quenching. Samples were incubated at temperatures above the lipid's phase-transition temperature for 2 h and then extruded at this elevated temperature through 100 nm pore size membranes in a hand extruder or a thermobarrel extruder (Lipex Biomembranes, Vancouver, BC) to produce large unilamellar vesicles (LUVs). Free SRB was removed by size exclusion chromatography on a prewarmed BioGel A15M using prewarmed 20 mM HEPES, pH 7.0, with 100 mM NaCl or

10 mM EDTA and 90 mM NaCl as the eluting solvent. LUVs consistently eluted in the void volume as a pink band. Encapsulation was tested by monitoring fluorescence at 560 nm excitation and 590 nm emission at temperatures above the lipid phase-transition temperature both before and after the addition of 2% sodium deoxycholate.

Cephaloridine Permeability. The cephaloridine permeabilities through bilayers composed of phospholipids or Rc or Rd LPS were determined by encapsulating *E. cloacae* β-lactamase within LUVs composed of those lipids. Films of acidified LPS (prepared as described above) were suspended in either 20 mM HEPES, 10 mM EDTA, and 90 mM NaCl, pH 7.0 (for the sodium salt form), or 0.2 molar equiv of $MgCl_2$ at a concentration of 0.5 mM $MgCl_2$, 20 mM HEPES, and 90 mM NaCl, pH 7.0 (for the partial magnesium salt form) containing between 5 and 15 mg/mL *E. cloacae* β-lactamase (*5*). The resulting multilamellar vesicle preparations were heated to 37 °C, hydrated, and converted to LUVs as described above, and separated from unincorporated β-lactamase by gel filtration on BioGel A15M at 37 °C. Permeability to cephaloridine was measured by the method of Yamaguchi et al. (*30*) by adding 454 μM cephaloridine as well as a 0.2% starch iodide complex to the outside of LUVs containing the entrapped β-lactamase. The rate of the enzymatic reaction was followed by monitoring the decrease in absorbance at 620 nm following reaction of the hydrolyzed β-lactam with the starch iodide. The rate of reaction of disrupted liposomes was measured after the addition of 0.5% Triton X-100.

A permeability parameter (P) was calculated, based on the approach of Zimmermann and Rosselet (*2*), that notes when the β-lactam antibiotic reaches the encapsulated β-lactamase by diffusion, the rate of diffusion and the velocity of antibiotic hydrolysis are equal at steady state, so that

$$P = (1/(S_o - S_i))(V_{max}S_i/(K_m + S_i))(1/A) \qquad (1)$$

where S_o is the concentration of antibiotic outside the liposomes, S_i is the concentration of antibiotic inside the liposomes, V_{max} is the maximum enzyme velocity, K_m is the binding constant of the enzyme (measured to be 456 μM for *E. cloacae* β-lactamase), and A is the bilayer area in the assay. To determine bilayer area, we used an average area per molecule of 60 Å^2 for the phospholipids and an area of 160 Å^2 for LPS (*6*). To determine S_i, we used the following formula, derived from the Michaelis−Menton equation by Sawai et al. (*31*), and used by Yamaguchi et al. (*30*) and Sawai et al. (*31*) in their membrane permeability measurements of β-lactams:

$$S_i = v_i/v_d[K_mS_o/(K_m + S_o - S_ov_i/v_d)] \qquad (2)$$

where v_i and v_d are reaction velocities (obtained from plots of cephaloridine hydrolysis versus time) for intact and detergent-disrupted LUVs, respectively.

Nitrocefin Permeability. Nitrocefin permeabilities through bilayers were measured by incorporating the *B. cereus* type II β-lactamase in LUVs. Because this β-lactamase is stable at temperatures up to 45 °C, all LPSs, including Ra LPS, could be used to encapsulate this enzyme. Sodium-salted vesicles were made by hydrating 2−5 mg of LPS or lipid at 45 °C for at least 2 h in 20 mM HEPES, 90 mM NaCl, and 10 mM $ZnSO_4$, containing 0.3 mg/mL *B. cereus* type II β-lactamase, whereas Mg-salted vesicles were made with 0.6 mg/mL lactamase and 0.2 molar equiv of $MgCl_2$ at a concentration of 0.5 mM in 20 mM HEPES, 90 mM NaCl, and 10 mM $ZnSO_4$. The material was then extruded as above. Sodium salt form LUVs had excess enzyme inactivated by the addition of prewarmed 10 mM EDTA. LUVs were purified as in the cephaloridine permeability experiments. Permeability was assayed in 45 °C holding cells by adding 0.25 mL of sample to 0.75 mL prewarmed 100 μM nitrocefin in 20 mM HEPES, and 100 mM NaCl, pH 7.0, and monitoring the change in absorbance at 486 nm. LUVs were disrupted by the addition of 0.5% Triton X-100. The permeability parameter for nitrocefin was calculated with eqs 1 and 2 and a measured K_m of 7.26 μM for *B. cereus* type II β-lactamase.

Kinetics of BANS Binding. The rate of binding of the membrane fluorescent probe BANS was measured with an Applied Photosystems stopped-flow fluorometer that monitored the increase in fluorescence of 5 μM BANS in buffer (either 20 mM HEPES, 10mM EDTA, and 90 mM NaCl, pH 7.0, or 0.5 mM $MgCl_2$, 20 mM HEPES, and 90 mM NaCl, pH 7.0) added to 500 μM lipid in the form of extruded LUVs in the same buffer. Emission was monitored using a 450 nm cutoff filter and an excitation wavelength of 401 nm. Data were analyzed using the SX18MV software version 4.0 or using the nonlinear curve fit option on Kaleidagraph v3.0.8d.

Phosphate Assays. Lipid levels in LUVs were quantitated by phosphate assay (*32*).

X-ray Diffraction. X-ray diffraction experiments were performed on bacterial phospholipids by methods previously used to study the organization of hydrated LPS (*6*). BPL suspensions were prepared by extensively vortexing the dried lipids with excess amounts of the same buffers used in the permeability experiments. Experiments were also performed with these buffers containing various concentration of the large neutral polymer poly(vinylpyrrolidone) (PVP). The addition of PVP applies osmotic stress, concentrating and ordering the lipid arrays, and thereby allowing for sharp X-ray reflections (*33*). The lipid suspensions were sealed in quartz glass X-ray capillary tubes and mounted in a temperature-controlled chamber in a point-collimation X-ray camera. X-ray patterns were recorded on Kodak DEF X-ray film in a flat-plate film cassette.

RESULTS

Antibiotic Susceptibilities. Figure 2 shows the susceptibilities to novobiocin, nitrocefin, and cephaloridine of *E. coli* D21 (Ra), *S. typhimurium* SL848 (Rc P$^+$), *E. coli* D21e7 (RcP$^-$), and *E. coli* D21f (Rd P$^-$). The largest of these antibiotics, novobiocin, showed minimum inhibitory concentration (MIC) values in excess of 200 μg/mL for both of the rough strains (Ra and Rc P$^+$) but required only a concentration of 8−16 μg/mL to inhibit growth for the two deep rough bacteria (Rc P$^-$ and Rd P$^-$). These results were similar to those of Roantree et al. (*20*). Nitrocefin also showed an ability to discriminate between rough and deep rough strains. Cephaloridine, the smallest of the three antibiotics, showed no significant difference in its ability to inhibit growth of either rough or deep rough bacteria.

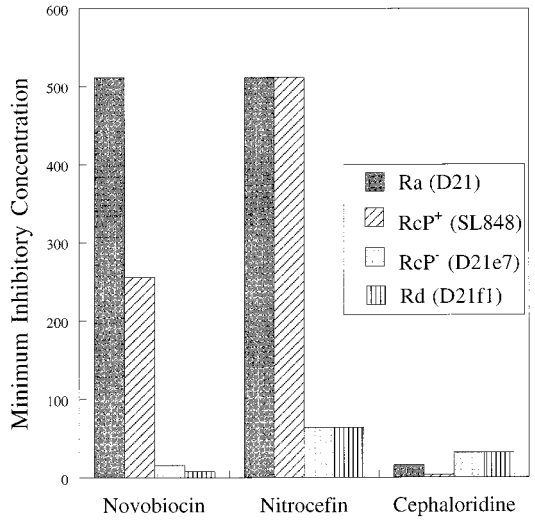

FIGURE 2: Susceptibilities of four bacterial strains to the hydrophobic antibiotics novobiocin, nitrocefin, and cephaloridine. The minimum inhibitory concentrations are given in units of micrograms per milliliter of antibiotic. Ra (D21) and RcP^+ (SL848) are rough phenotypes, whereas RcP^- (D21e7) and Rd (D21f1) are deep rough phenotypes.

Sulforhodamine B (SRB) Encapsulation. A prerequisite for the testing of bilayer permeability is the ability to form closed liposomes. We have tested for this by the encapsulation of SRB, a dye which is fluorescent at low concentrations but essentially self-quenching at concentrations higher than 1 mM (data not shown). In our hands, bacterial phospholipids (BPL) and all LPS chemotypes tested were capable of forming vesicles which could encapsulate this dye and which were stable for several days. Two requirements were noted for the formation of stable vesicles. First, all work had to be done at temperatures above the lipid phase-transition temperature. At 37 °C, SRB could be encapsulated in LUVs composed of all LPSs tested, except for Ra LPS which melts at approximately this temperature (*15*, *16*). However, for Ra LPS SRB encapsulation could be accomplished by increasing the temperature to 45 °C. Second, the buffer had to contain less than millimolar levels of divalent cations. Previous work (*6*) has shown that divalent cations are capable of mediating adhesion between LPS bilayers when present in molar excess and at 10 mM concentration. Although stable bilayers were still formed under these conditions, the lack of fluid space between bilayers prohibited solute encapsulation.

For all LPS chemotypes, a pattern of encapsulation similar to the one seen in Figure 3 was observed. Specifically, for SRB encapsulated in the LUV, there was a prolonged period of slow increase in SRB fluorescence, with an abrupt 3- to 5-fold increase in fluorescence after treatment with detergent.

Cephaloridine Permeability. Observed reaction velocities of cephaloridine hydrolysis, which were typically 5 to 10-fold lower in intact vesicles (v_i) than in detergent-disrupted vesicles (v_d), were used to estimate the permeability parameter (*P*) by the use of eqs 1 and 2. Figure 4 shows the permeability parameters for LUVs prepared from BPL, a series of LPS samples, and a BPL/Rd LPS mixture containing 30 area % (approximately 60 mol %) BPL, similar to the amount of phospholipids found on the surface of deep rough bacteria (*19*). For both the sodium and magnesium salt forms, the permeability parameters were lower for all of the LPSs

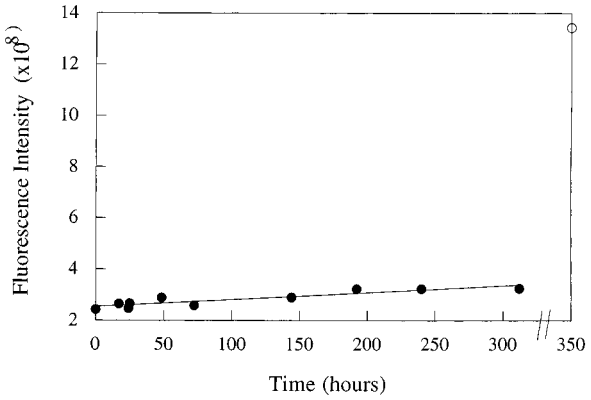

FIGURE 3: Fluorescence versus time for the fluorescent probe sulforhodamine B encapsulated in Rd (R7) LPS vesicles. The open circle on the right-hand vertical axis represents a reading after treatment of the vesicles with detergent (2% deoxycholate).

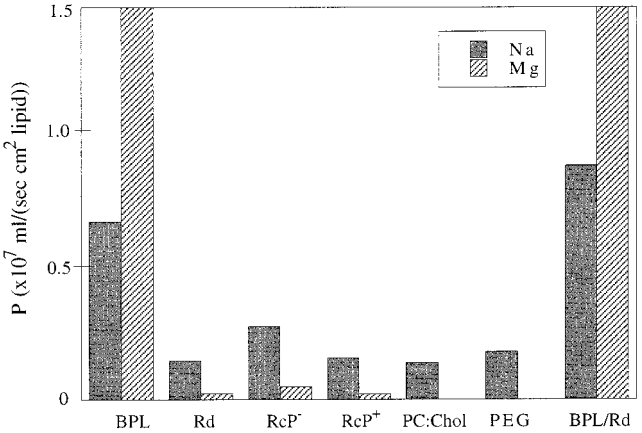

FIGURE 4: Permeability parameters (*P*) for cephaloridine through vesicles composed of BPL, Rd (D21f1) LPS, RcP^- (D21e7) LPS, RcP^+ (SL848) LPS, 7:3 DMPC/cholesterol, 6:3:1 DMPC/cholesterol/PEG−lipid, and a mixture of BPL with 70 area % Rd LPS. The values of *P* for BPL and BPL/Rd LPS in the magnesium salt form were off this scale, at $P = 4.6 \times 10^{-7}$ mL/(s·cm^2 lipid) and 2.0×10^{-7} mL/(s·cm^2 lipid), respectively.

tested than for BPL or the Rd LPS/BPL mixture. All sodium-salted LPS bilayers, regardless of chemotype, had a permeability parameter of $1-3 \times 10^{-8}$ mL/s·cm^2, significantly lower than the permeability of bacterial phospholipid bilayers in the absence of divalent cations (Figure 4). All LPS samples, either derived from rough (Rc P^+) or deep rough (Rc P^-, Rd) strains of bacteria, decreased their permeability to a level of $2-5 \times 10^{-9}$ cm^3/s·cm^2 when in a partial magnesium salt form (Figure 4). The BPL samples showed the reverse pattern, increasing their permeability in the presence of divalent cations to approximately 100 fold that of the LPS bilayers.

As additional control experiments, we determined the cephaloridine permeability to vesicles composed of a 7:3 mol/mol mixture of DMPC/cholesterol and a 6:3:1 mol/mol/mol mixture of DMPC/cholesterol/PEG−lipid (PEG-2000). DMPC was chosen at it has the same number of carbon atoms in its hydrocarbon chains (*14*) as that found in most of the fatty acid chains in LPS. This concentration of PEG-2000 is large enough so that the "brush" regime of extended PEG polymers is formed around the liposomal surface (*8*). The permeabilities of both the DMPC/cholesterol and

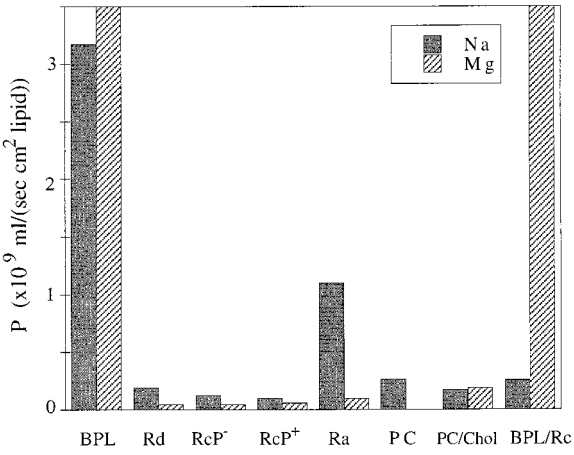

FIGURE 5: Permeability parameters for nitrocefin through vesicles composed of BPL, Rd (D21f1) LPS, RcP$^-$ (D21e7) LPS, RcP$^+$ (SL848) LPS, Ra (D21) LPS, DMPC, 7:3 DMPC/cholesterol, and a mixture of BPL with 70 area % RcP$^+$ LPS. The values of P for BPL and BPL/Rc LPS in the magnesium salt form were off this scale, both at $P = 2.0 \times 10^{-8}$ mL/(s·cm^2 lipid).

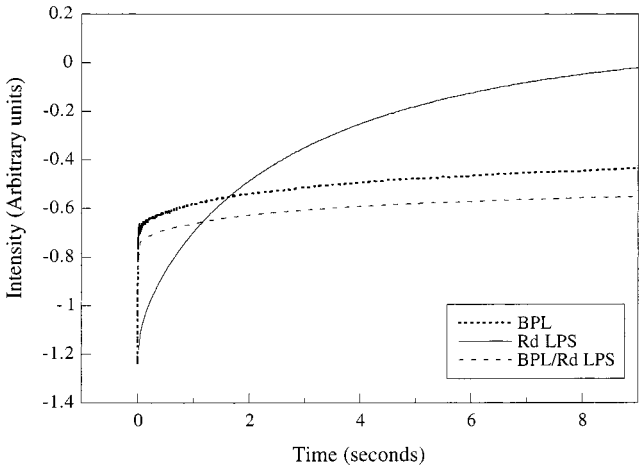

FIGURE 6: Typical experiments showing the kinetics of BANS binding to large unilamellar vesicles composed of Rd (R7) LPS (solid line), BPL (dotted line), and a mixture of BPL with 30 area % Rd (R7) LPS (dashed line) all in 90 mM NaCl in the absence of $MgCl_2$.

DMPC/cholesterol/PEG−lipid vesicles were similar to those of LPS in the sodium salt form, and considerably larger than LPS in the magnesium salt form.

Nitrocefin Permeabilities. Figure 5 shows the nitrocefin permeability parameters of bilayers composed of BPL, dimyristoylphosphatidylcholine (DMPC), a 7:3 DMPC/cholesterol mixture, and LPSs derived from various rough and deep rough bacteria. The permeabilities of LPS bilayers derived from both rough (Ra, RcP$^+$) and deep rough (RcP$^-$, RdP$^-$) chemotypes were lower than those obtained for bilayers of BPL. Addition of $MgCl_2$ decreased permeability of all LPS chemotypes tested, had no appreciable effect on the permeability of DMPC/cholesterol bilayers, and increased BPL bilayer permeability. Addition of BPL to magnesium-salted LPS bilayers at a level observed in deep rough mutants increased permeability to the level observed for the phospholipids alone.

Binding of BANS to Lipid Bilayers. As shown in Figure 6, when BANS was mixed with bacterial phospholipids in a stopped-flow fluorometer, rapid binding was observed with most of the reaction completed within 0.2 s, although there was slower increase in fluorescence for longer times. BANS binding was much slower to bilayers of LPS in either the sodium (Figure 6) or magnesium salt forms (data not shown). The addition of phospholipids to the LPS bilayers increased the rate of increase in fluorescence to a rate similar to that observed with the phospholipids (Figure 6).

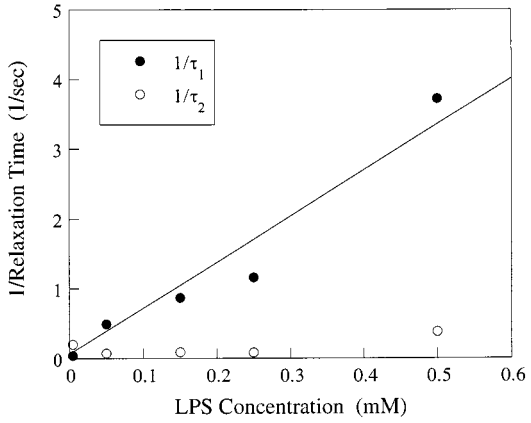

FIGURE 7: Inverse of the BANS relaxation times ($1/\tau_1$ and $1/\tau_2$) versus lipid concentration for Rd (R7) LPS. The solid line is a least-squares fit to the data for the first relaxation time.

To analyze the BANS binding data, we fit the data with a double-exponential rate equation, with τ_1 and τ_2 representing relaxation times of a relatively fast and a slower process, respectively. The use of a single-exponential rate equation gave a poorer fit, with a 10-fold higher variance (data not shown). To determine rate constants (k_1 and k_2) for BANS binding, we followed a procedure similar to that of Clarke and Apell (*26*) and measured BANS finding for several lipid concentrations. A plot of $1/\tau_1$ versus lipid concentration produced a straight line with a near-zero y-intercept, whereas a plot of $1/\tau_2$ was nearly independent of lipid concentration (Figure 7). Therefore, as found by Clarke and Apell (*26*) for the interactions of fluorescent dyes with lipid bilayers, the fast process most likely represents a binding event, whereas the slower process probably represents a change in probe orientation or position in the bilayer. The pseudo-first-order rate constant k_1 was obtained by dividing $1/\tau_1$ by the molar concentration of lipid (*34*), and the first-order rate constant k_2 was set equal to $1/\tau_2$ (*26*, *34*). These rate constants for the fast (k_1) and slower (k_2) processes are given in Table 1, and k_1's for several lipids are also plotted in Figure 8 for ease of comparison.

The first-order rate constants were significantly lower for LPS bilayers than those for phospholipid bilayers (Table 1, Figure 8). For instance, there was approximately 2 orders of magnitude difference in k_1 for Rd LPS in the sodium salt form compared to that for BPL. The k_1 for Ra LPS at 45 °C was somewhat higher than that for Rd LPS at this temperature. Because the phase transition for Ra LPS is quite broad and centered near 37 °C (*15*, *16*), we were concerned that there might be a mixture of gel and liquid-crystalline phase present at 45 °C. Therefore, we performed additional experiments at 50 °C. At this elevated temperature, the k_1 value for Ra LPS was somewhat reduced and comparable to the value for Rd LPS at this temperature. The values of k_1 increased with increasing concentration of BPL in the bilayer (Table 1, Figure 8).

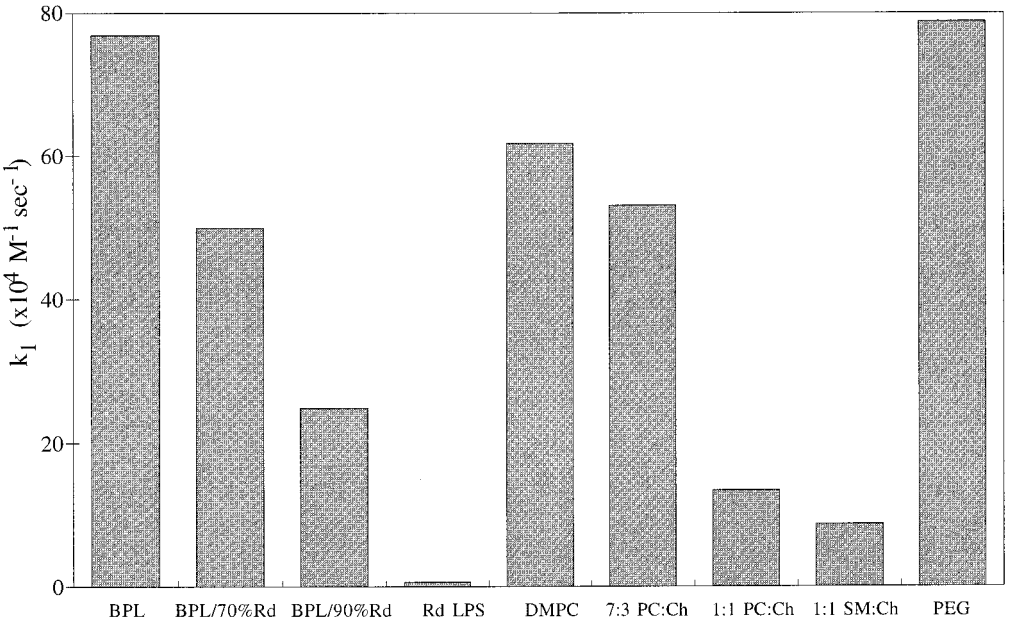

FIGURE 8: Pseudo-first-order rate constants (k_1) for BANS binding to unilamellar bilayers composed of BPL, BPL with 70 area % Rd LPS, BPL with 90 area % LPS, Rd LPS, DMPC, 7:3 molar ratio DMPC/cholesterol, equimolar DMPC/cholesterol, equimolar SM/cholesterol, and 6:3:1 DMPC/cholesterol/PEG−lipid.

Table 1: BANS Binding Kinetics[a]

lipid	k_1 ($\times 10^4$ s^{-1} M^{-1})	k_2 (s^{-1})
Phospholipid/Cholesterol		
BPL	76.9	0.6
DMPC	61.8	5.2
7:3 DMPC/Chol	53.1	1.7
1:1 DMPC/Chol	13.4	0.3
1:1 SM/Chol	8.7	0.2
6:3:1 DMPC/Chol/DPPG	61.0	4.3
6:3:1 DMPC/Chol/PEG-2000	78.8	1.0
LPS		
Rd LPS Na	0.7	0.3
Rd LPS Na (50 °C)	0.2	0.3
Rd LPS Mg	0.7	0.3
Ra LPS Mg	5.6	0.1
Ra LPS Na (50 °C)	1.1	0.3
Ra LPS Mg (50 °C)	0.3	0.3
Phospholipid/LPS		
BPL/70 area% Rd LPS Na	50.0	0.8
BPL/90 area% Rd LPS Na	24.9	1.0

[a] Experiments were performed at 45 °C unless otherwise noted.

Control experiments showed that k_1 for DMPC was somewhat lower than that of BPL. The addition of increasing concentrations of cholesterol to DMPC reduced the observed value of k_1 (Table 1, Figure 8). Experiments with an equimolar mixture of sphingomyelin (SM) and cholesterol, a bilayer with a very large area expansion modulus (*35*), also had a relatively low value of k_1 (Table 1, Figure 8). However, the introduction of 10 mol % of a phospholipid containing a covalently attached PEG chain (PEG-2000) produced no appreciable change in k_1. Since PEG-2000 is negatively charged, we tested the effect of negative charge on k_1 by incorporating 10 mol % dipalmitoylphosphatidylglycerol (DPPG) into DMPC/cholesterol bilayers. This incorporation of DPPG also had no appreciable effect on k_1 (Table 1).

X-ray Diffraction. At 37 °C, total *E. coli* phospholipids in 20 mM HEPES, 10 mM EDTA, and 90 mM NaCl, pH 7.0, gave a diffraction pattern consisting of a broad band centered at 0.025 $Å^{-1}$, typical of the Fourier transform of lipid bilayers with indefinitely large interbilayer fluid spacings (*33*). The large fluid spacings with these native lipid mixtures were undoubtedly caused by the presence of phospholipids with a net negative charge. Upon the addition of 34% PVP, the pattern consisted of several sharp reflections that indexed as orders of a lamellar diffraction pattern with a repeat period of 53 Å. Similar results were obtained with these *E. coli* phospholipids in 20 mM HEPES, 0.5 mM $MgCl_2$, and 90 mM NaCl; in the absence of PVP, a broad low-angle band was observed at 0.025 $Å^{-1}$, whereas in the presence of PVP, sharp low-angle reflections were observed that indexed as orders of a lamellar repeat period. Similar results were also obtained with the *E. coli* phospholipids supplemented by 4 mol % cardiolipin, as used in the permeability experiments. Thus, at 37 °C, the bacterial phospholipids in either 0 or 0.5 mM $MgCl_2$ gave diffraction patterns consistent with bilayer (lamellar) phases. However, the presence of higher concentrations of $MgCl_2$ produced different X-ray results. At 45 °C in the presence or absence of PVP, in 10 mM $MgCl_2$ the bacterial phospholipids gave sharp reflections that indexed as a hexagonal phase with a primary spacing of 60 Å, whereas at 37 °C, the pattern contained two sets of reflections, one indexing as orders of a lamellar lattice and the other indexing as orders of a hexagonal phase.

DISCUSSION

Correlation of the susceptibility, permeability, and BANS kinetic binding data allows us to test several hypotheses concerning the mechanism of the permeability barrier provided by LPS in the outer monolayer of the bacterial outer membrane and to obtain insights as to the molecular mechanisms involved in the permeability barrier provided by LPS.

Antibiotic Susceptibilities. The three antibiotics tested in this study showed a size-dependent ability to differentiate between deep rough and rough bacteria. For the largest

antibiotic, novobiocin, deep rough bacteria were significantly more susceptible than the rough chemotypes (Figure 2), a pattern of resistance similar to that observed by Roantree et al. (*20*) for this antibiotic. The only notable difference between strains was the increased susceptibility of the Rc P^+ strain SL848, which may reflect a higher intrinsic susceptibility of this organism to this type of antibiotic. Cephaloridine, the smallest of the three antibiotics, had a similar effect on growth inhibition for rough and deep rough bacteria. The similarity in susceptibilities to cephaloridine of rough and deep rough support the idea that this small antibiotic can enter into the cells through porin channels (*24*). Nitrocefin, of intermediate size between novobiocin and cephaloridine, inhibited growth of deep rough more than rough bacteria, although to a somewhat smaller extent than that for novobiocin. This may indicate that nitrocefin has some ability to penetrate through porin channels, but that the LPS-based permeability barrier plays a role in preventing this molecule from entering the cell.

Antibiotic Permeability. Under the conditions used in these experiments, sodium-salted and partially magnesium-salted LPS formed sealed vesicles that encapsulated solute (Figure 3**)**, allowing measurements of bilayer permeability. For nitrocefin and cephaloridine, the overall pattern of permeabilities of the different LPS and phospholipid bilayers were similar (Figures 4 and 5). That is, despite differences in the assay system and enzyme used, LPS bilayers consistently had lower permeabilities than those of bacterial phospholipid bilayers, and the addition of $MgCl_2$ reduced the LPS permeability even further but raised the permeability of BPL bilayers. For both cephaloridine and nitrocefin, the permeabilities of the partially magnesium-salted LPS samples were some 2 orders of magnitude less than the permeability of either bacterial phospholipids by themselves or when mixed with LPS at a 30 area % level. Pleisat and Nikaido (*21*) noted a similar difference in the permeability of steroids through intact bacteria when they compared rough and deep rough strains. The one exception to this was the relatively high permeability to nitrocefin of Ra LPS (Figure 5). This sample showed a reduction in permeability with the addition of magnesium, but the permeability parameter for the sodium salt was significantly higher than those for the other LPS samples. One possible explanation of this observation is that even at 45 °C there might be a small amount of gel phase in the Ra LPS sample, which has a very broad phase transition centered at 37 °C (*16*). Due to packing defects, the permeability might be larger for bilayers containing mixtures of gel and liquid-crystalline phase lipids.

Previous studies by Hiruma et al. (*5*) measured the cephaloridine permeability of BPL liposomes at room temperature containing relatively small amounts of LPS (0−15 mol % LPS). These small concentrations of LPS decreased permeability. However, unlike our results (Figure 4), Hiruma et al. (*5*) did not observe an increase in the permeability to cephaloridine of BPL bilayers upon addition of excess magnesium. A difference in these results may stem from the thermal properties of BPL and the fact that our studies were performed at 37 °C, whereas the Hiruma et al. studies were performed at room temperature. NMR methods (*36*) have shown that, in the presence of EDTA, bacterial phospholipids undergo a broad bilayer-to-hexagonal phase transition between 50 and 60 °C. Our X-ray results showed that, although bilayers were formed under the experimental conditions used in our permeability experiments, depending on the temperature, hexagonal or mixed hexagonal-bilayer phases were formed at higher concentrations of $MgCl_2$. Bentz et al. (*37*) have found that lipids that form hexagonal phases at elevated temperatures are leaky at temperatures a few degrees below their lamellar-to-hexagonal phase transition. Therefore, the high permeability of BPL in our experiments, particularly in the presence of magnesium, may be due to the leakiness of these bilayers at temperatures below the bilayer-to-hexagonal phase transition. We note that, unlike BPL, the nitrocefin permeability of DMPC/cholesterol bilayers was not changed appreciably by the presence of magnesium. DMPC/cholesterol forms stable bilayers over a wide range of ionic conditions and temperatures.

Another similarity between the cephaloridine (Figure 4) and nitrocefin (Figure 5) permeability experiments was that in the magnesium salt form LPS samples showed extremely high levels of permeability to both antibiotics in the presence of the amount of phospholipids (30 area %) observed on surface of deep rough mutants (*19*). Smooth and rough chemotypes have significantly lower levels of phospholipids in the outer monolayers of their outer membranes (*19*). This increase in antibiotic permeability in the presence of magnesium was observed upon phospholipid addition to either rough (RcP^+, see Figure 5) or deep rough (Rd, see Figure 4) LPS, suggesting that the mixture of phospholipids and LPS, independent of the LPS chemotype, is responsible for the increase in permeability. We have no explanation for the relatively low permeability to nitrocefin of the BPL/Rc mixture in the sodium salt form.

Fluorescent Probe Binding Kinetics. In addition to limiting passage across their outer membrane, bacteria also need to prevent access to this membrane for a number of agents such as detergents and lipases. The significantly smaller BANS binding rates (k_1) we observed for both deep rough and rough LPS bilayers compared to BPL and other phospholipid bilayers (Table 1) make sense in this light.

The kinetics of binding of BANS allows us to model as chemical reactions both passage into the bilayer (k_1) and movement within the bilayer (k_2). This is similar to the approach of Kleinfeld (*38, 39*) that treats permeability of fatty acids across bilayers as a function of an on-rate, a flip-flop rate, and an off-rate, as well as the model of Clarke and Apell (*26*) that treats the interaction of the hydrophobic dye oxonol with bilayers in terms of a fast-binding step and a slower step related to position of probe in the bilayer or diffusion through the bilayer. For example, k_2 could represent movement of BANS either from the bilayer interface to the center of the bilayer or diffusion through the bilayer core. If these models (*26, 38, 39*) were correct, increasing the tightness of lipid packing in the plane of the bilayer should reduce diffusion through the bilayer. Indeed, the slow rate (k_2) in this model decreased with increasing concentrations of cholesterol in the bilayer (Table 1). However, it should be noted that in these kinetic experiments we collected a significantly larger number of data points for small times, making our values of k_1 more reliable than our values of k_2.

We now consider the molecular factors that are involved in the binding step (k_1). A solubility-diffusion model would treat passage through the LPS sugar core in terms of diffusion through a saccharide solution on the surface of the bilayer.

However, even a densely intertwined polysaccharide matrix would reduce diffusion by only 3% for small molecules (*4*), far less than what is needed to account for the difference in k_1 between BPL and LPS bilayers (Table 1). Further, if diffusion to the bilayer interface were the limiting factor for the on-rate, bilayers with PEG−lipid would be expected to show a reduction in this reaction rate as well. They did not (Table 1). Moreover, the range of the steric barrier for 10 mol % PEG-2000 used in our experiments (Figure 4 and Table 1) is much larger (*8*) than the range of the steric barrier for any of the rough or deep rough LPSs (*6*). Therefore, in agreement with Nikaido and Vaara (*4*), we argue that the observed differences in binding rate of BANS to LPS bilayers compared to phospholipid bilayers cannot be due to slow diffusion of BANS through the LPS oligosaccharide core.

Instead, the rate reduction is likely to be due, at least in part, to tight packing of the LPS molecules within the bilayer. Previously we found that the area per hydrocarbon chain in liquid-crystalline LPS bilayers is only about 26 Å^2 (*6*), a value considerably smaller than the values of 32−41 Å^2 observed for membrane phospholipids (*40*−*43*). Consistent with this proposed role of the tight chain packing in the outer bacterial monolayer is the observation of Wiese et al. (*44*) on the glycolipid component of the Gram-negative bacterium *Spingomonas paucimobilis*. This species does not contain LPS in its outer monolayer, but instead contains a glycosphingolipid (GSL-1) that, like LPS, has a very small area per hydrocarbon chain in monolayers (*44*). Also consistent are the observations that addition of cholesterol decreased permeability (Figure 4) and decreased the rate of BANS binding (Table 1, Figure 8) to DMPC bilayers. Cholesterol is known to decrease the area per lipid molecule in bilayers and increase the elastic area expansion modulus (a measure of the pressure required to move the molecules apart in the plane of the bilayer) (*35*).

Although our data cannot distinguish between area per molecule and expansion coefficient as being more important for a reduction in permeability, it is tempting to speculate that the intermolecular attractive forces which lead to a small area per molecule also lead to an increase in the energy required to push the molecules in the membrane apart, as would be necessary to form the k_1 transition state. Needham and Nunn (*35*) have shown with PC/cholesterol bilayers that there is a strong correlation between high elastic area expansion modulus and small area per molecule. We argue that the small area per hydrocarbon chain in LPS bilayers is due to the fact that these lipids have saturated hydrocarbon chains and that there are strong attractive forces between the sugar cores. Previous work (*45, 46*) suggests that the headgroups on glycolipids mediate strong attractive intermolecular forces both between and within the bilayers. The presence of magnesium would be expected to further decrease the area per chain (and thereby decrease permeability and decrease binding rate constants) by neutralizing the electrostatic repulsion between the negatively charged LPS molecules. Our previous X-ray experiments were not sensitive enough to record such a decrease in area with divalent cations (*6*). However, a quite small area decrease can cause a relatively large increase in area compressibility modulus (*35*).

Therefore, as part of its role in Gram-negative bacteria, LPS could provide an effective permeability barrier due to its tight intermolecular packing in the plane of the bilayer. Thus, LPS could serve a role for bacteria similar to that cholesterol serves in eukaryotic membranes. Cholesterol, found in high concentrations in eukaryotic plasma membranes, reduces the area per lipid molecule in the bilayer (*47*) and reduces bilayer permeability (*48, 49*). LPS bilayers have a smaller area per hydrocarbon chain than do equimolar phospholipid/cholesterol bilayers (*6*) and have a much lower permeability to hydrophobic antibiotics than bacterial phospholipid bilayers, and a somewhat lower permeability than even PC/cholesterol bilayers (Figures 6, 7).

Evaluation of Hypotheses Regarding Susceptibility/Permeability. As noted in the Introduction, there are several models for the function of the LPS-based permeability barrier. We will now consider each of these in turn.

If the permeability barrier of LPS were mediated solely through its carbohydrate chain, the permeabilities of deep rough LPS bilayers should be greater than those of rough LPS bilayers and there should be no difference in permeability with added divalent cations. Clearly, this was not the case, as neither cephaloridine nor nitrocefin showed such a pattern. Indeed, the deep rough LPS permeabilities were comparable to those of rough LPS (Figures 6 and 7). Further, as determined previously (*6*), there was no difference in the core width between the RcP$^+$ and RcP$^-$ LPS samples even though there are profound differences in the susceptibilities of these two strains to novobiocin (Figure 2). Moreover, as noted above, the role of a hydrophobic shield was tested by adding PEG−lipids to phospholipid bilayers. Our experiments showed that the addition of PEG−lipids had little effect on permeability (Figure 4) or the kinetics of BANS binding to phospholipid bilayers (Table 1).

The interaction of LPS with divalent cations has also been invoked as a factor in the permeability barrier of the outer membrane (*3*). Divalent cations did indeed decrease LPS bilayer permeability, even at the low divalent cation concentrations used in our studies (Figures 6 and 7). It is reasonable to assume that in a natural environment, the bacterial cell surface is exposed to divalent cations, and it has been found that divalent cations bind to the inner core region of the LPS headgroup (*6*). Galanos and Luderitz (*12*) show that LPS isolated from *S. minnesota* R5 has 0.195 mM Mg^{2+} and 0.05 mM Ca^{2+} for 0.03 mM LPS. This means that the permeability of LPS on the surface of the bacteria is likely to be at least as low as that determined for our partially magnesium-salted samples. In the presence of magnesium, bilayers composed of all LPSs tested, including those from deep rough chemotypes, were much less permeable than BPL (Figures 6 and 7). Although these observations may help explain how LPS acts as a permeability barrier, they do little to explain the higher susceptibility of the deep rough compared to rough bacteria (Figure 1), as both rough and deep rough chemotypes bind divalent cations.

Interactions between polar substituents do not seem to account for susceptibility increases in deep rough bacteria. Both of the heptose phosphate-deficient LPSs (Rd and RcP$^-$) showed permeabilities similar to those of the heptose phosphate-positive LPSs (Ra and RcP$^+$; see Figures 6 and 7).

The hypothesis that the permeability barrier of LPS is related to its gel to liquid crystalline phase-transition temperature (*15*) is unable to explain several experimental observations. First, certain rough (Rc P$^+$) and deep rough

(Rc P$^-$ and Rd) LPSs have similar phase-transition temperatures and similar permeabilities at physiological temperature (37 °C), even though the intact bacterial chemotypes have very different susceptibilities (Table 1). Moreover, the decrease in LPS permeability with the addition of divalent cations for all LPSs tested (Figures 6 and 7) is not explained by this hypothesis, as these cations have a larger effect on the phase transition of LPSs with shorter sugar chains than the Ra chemotype (*16*).

The phospholipid exclusion hypothesis of Nikaido and colleagues (*4*, *18*) appears to be consistent with all of our observed data. When phospholipid was added to LPS bilayers at levels similar to those observed on the cell surface of deep rough mutants (*19*, *50*), the permeability (Figures 6 and 7) and binding rate constant (k_1 in Table 1) both increased dramatically. Moreover, the effects of divalent cations on LPS permeability were negated by the addition of phospholipids to the LPS bilayers. We argue that the phospholipid exclusion hypothesis adequately explains the observed differences in susceptibility between rough and deep rough bacterial chemotypes.

Unknown is the mechanism by which the addition of phospholipid increases the permeability of LPS bilayers. One possibility is that patches of exposed phospholipid could be formed in the LPS bilayer (*51*), thereby providing a low permeability region in the LPS barrier (*20*). A second possibility is that the phospholipid and LPS could mix, with the phospholipid modifying the LPS packing properties. In this second model, the presence of phospholipids between adjacent LPS molecules could act as a spacer in the plane of the bilayer, reducing the short-range attractive forces between LPS saccharide cores. This would cause an increase in the area per hydrocarbon chain and a decrease in the area expansion modulus. The resolution of this mechanistic question awaits additional experiments.

SUMMARY

LPS from both rough and deep rough chemotypes form bilayers with relatively low permeabilities to hydrophobic antibiotics, particularly in the presence of magnesium. This low permeability is most likely due to the very tight packing of the LPS molecules in the plane of the bilayer *(6)*, caused by intermolecular acyl chain and saccharide−saccharide interactions. The antibiotic permeability and rate of probe binding both increase when phospholipids are added to the LPS bilayers. We argue that the greater susceptibilities of deep rough compared to rough bacteria are due to the presence of phospholipid on the surface of these bacteria.

ACKNOWLEDGMENT

We thank Drs. A. Gal and J. S. Stamler for the use of the stopped-flow fluorometer, Dr. H. P. Erickson for the use of his spectrophotometer, and Drs. M. Galleni and J. Fralick for the generous gifts of β-lactamase and bacterial strains, respectively.

REFERENCES

1. Nikaido, H. (1994) *Science 264*, 382−388.
2. Zimmermann, W., and Rosselet, A. (1977) *Antimicrob. Agents Chemother. 12*, 368−372.
3. Hancock, R. E. W. (1984) *Annu. Rev. Microbiol. 38*, 237−264.
4. Nikaido, H., and Vaara, M. (1985) *Microbiol. Rev. 49*, 1−32.
5. Hiruma, R., Yamaguchi, A., and Sawai, T. (1984) *FEBS Lett. 170*, 268−272.
6. Snyder, S., Kim, D., and McIntosh, T. J. (1999) *Biochemistry 38*, 10758−10767.
7. Needham, D., McIntosh, T. J., and Lasic, D. D. (1992) *Biochim. Biophys. Acta 1108*, 40−48.
8. Kenworthy, A. K., Hristova, K., Needham, D., and McIntosh, T. J. (1995) *Biophys. J. 68*, 1921−1936.
9. Kenworthy, A. K., Simon, S. A., and McIntosh, T. J. (1995) *Biophys. J. 68*, 1903−1920.
10. Needham, D., Stoicheva, N., and Zhelev, D. V. (1997) *Biophys. J. 73*, 2615−2629.
11. Stan-Lotter, H., Gupta, M., and Sanderson, K. E. (1979) *Can. J. Microbiol. 25*, 475−485.
12. Galanos, C., and Luderitz, O. (1975) *Eur. J. Biochem. 54*, 603−610.
13. Parker, C. T., Kloser, A. W., Schnaitman, C. A., Stein, M. A., Gottesman, S., and Gibson, B. W. (1992) *J. Bacter. 174*, 2525−2538.
14. Schnaitman, C. A., and Klena, J. D. (1993) *Microbiol. Rev. 57*, 655−682.
15. Brandenburg, K., and Seydel, U. (1984) *Biochim. Biophys. Acta 775*, 225−238.
16. Seydel, U., Koch, M. H. J., and Brandenburg, K. (1993) *J. Struct. Biol. 110*, 232−243.
17. Nikaido, H. (1976) *Biochim. Biophys. Acta 433*, 118−132.
18. Vaara, M., Plachy, W. Z., and Nikaido, H. (1990) *Biochim. Biophys. Acta 1024*, 152−158.
19. Kamio, Y., and Nikaido, H. (1976) *Biochemistry 15*, 2561−2569.
20. Roantree, R. J., Kuo, T.-T., and MacPhee, D. G. (1977) *J. Gen. Microbiol. 103*, 223−234.
21. Plesiat, P., and Nikaido, H. (1992) *Mol. Microbiol. 6*, 1323−1333.
22. Negrete, H. O., Rivers, R. L., Gough, A. H., Colombini, M., and Zeidel, M. L. (1996) *J. Biol. Chem. 271*, 11627−11630.
23. Hill, W. G., Rivers, R. L., and Zeidel, M. L. (1999) *J. Gen. Physiol. 114*, 405−414.
24. Nikaido, H., Song, S. A., Shaktiel, L., and Nurminen, M. (1977) *Biochem. Biophys. Res. Commun. 76*, 324−330.
25. Haynes, D., and Simkowitz, P. (1977) *J. Membr. Biol. 33*, 63−108.
26. Clarke, R. J., and Apell, H.-J. (1989) *Biophys. Chem. 34*, 225−237.
27. Galanos, C., Luderitz, O., and Westphal, O. (1969) *Eur. J. Biochem. 9*, 245−249.
28. Qureshi, N., Takayama, K., Heller, D., and Fenselau, C. (1983) *J. Biol. Chem. 258*, 12947−12951.
29. Waitz, J. A., Doern, G. V., Finegold, S. M., Gavan, T. L., Hackett, J. L., Jones, R. N., Jorgensen, J. H., King, J. R., and Miller, G. H. (1990) *Methods for Dilution Antimicrobial Susceptibility Tests for Bacteria That Grow Aerobically*, 2nd ed., National Committee for Clinical Laboratory Standards, Villanova, PA.
30. Yamaguchi, A., Hiruma, R., and Sawai, T. (1982) *J. Antibiot. 34*, 1692−1699.
31. Sawai, T., Matsuba, K., and Yamagishi (1977) *J. Antibiot. 30*, 1134−1136.
32. Chen, P. S., Jr., Toribara, T. Y., and Warner, H. (1956) *Anal. Chem. 28*, 1756−1758.
33. McIntosh, T. J., and Simon, S. A. (1986) *Biochemistry 25*, 4058−4066.
34. Bunnett, J. F. (1986) Kinetics in Solution, in *Investigation of Rates and Mechanisms of Reactions*, Part 1 (C. F. Bernasconi, Ed.), 171−250, John Wiley and Sons, New York.
35. Needham, D., and Nunn, R. S. (1990) *Biophys. J. 58*, 997−1009.
36. Cullis, P. R., and DeKruijff, B. (1978) *Biochim. Biophys. Acta 513*, 31−42.
37. Bentz, J., Ellens, H., Lai, M.-Z., and Szoka, F. C. (1985) *Proc. Natl. Acad. Sci. U.S.A. 82*, 5742−5745.
38. Storch, J., and Kleinfeld, A. M. (1986) *Biochemistry 25*, 1717−1726.

39. Kleinfeld, A. M. (1995) Fatty Acid Transport Across Bilayers, in *Permeability and Stability of Lipid Bilayers*, 251−258, CRC Press, London.
40. Lis, L. J., McAlister, M., Fuller, N., Rand, R. P., and Parsegian, V. A. (1982) *Biophys. J. 37*, 667−672.
41. McIntosh, T. J., and Magid, A. D. (1993) Phospholipid Hydration, in *Phospholipid Handbook* (Cevc, G. Ed.) pp 553−577, Marcel Dekker, Inc., New York.
42. McIntosh, T. J., Advani, S., Burton, R. E., Zhelev, D. V., Needham, D., and Simon, S. A. (1995) *Biochemistry 34*, 8520−8532.
43. Petrache, H. I., Tristram-Nagle, S., and Nagle, J. F. (1998) *Chem. Phys. Lipids 95*, 83−94.
44. Wiese, A., Reiners, J. O., Brandenburg, K., Kawahara, K., Zahringer, U., and Seydel, U. (1996) *Biophys. J. 70*, 321−329.
45. Curatolo, W. (1987) *Biochim. Biophys. Acta 906*, 137−160.
46. Kulkarni, K., Snyder, D. S., and McIntosh, T. J. (1999) *Biochemistry 38*, 15264−15721.
47. Lecuyer, H., and Dervichian, D. G. (1969) *J. Mol. Biol. 45*, 39−57.
48. Papahadjopoulos, D., Cowden, M., and Kimelberg, H. (1973) *Biochim. Biophys. Acta 330*, 8−26.
49. Szabo, G. (1974) *Nature 252*, 47−49.
50. Smit, J., Kamio, Y., and Nikaido, H. (1975) *J. Bacteriol. 124*, 942−958.
51. Takeuchi, Y. and Nikaido, H. (1981) *Biochemistry 20*, 523−529.

BI000810N